NeuroImage 257 (2022) 119286

Contents lists available at ScienceDirect

NeuroImage

journal homepage: www.elsevier.com/locate/neuroimage

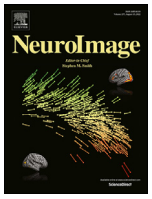

Combined analysis of cytoarchitectonic, molecular and transcriptomic patterns reveal differences in brain organization across human functional brain systems

Daniel Zachlod[a,*], Sebastian Bludau[a], Sven Cichon[a,d,e], Nicola Palomero-Gallagher[a,b,c], Katrin Amunts[a,b]

[a] Institute of Neurosciences and Medicine (INM-1), Research Centre Jülich, Jülich, Germany
[b] C. & O. Vogt Institute for Brain Research, Medical Faculty, University Hospital Düsseldorf, Heinrich-Heine University Düsseldorf, Düsseldorf, Germany
[c] Department of Psychiatry, Psychotherapy, and Psychosomatics, Medical Faculty, RWTH Aachen, and JARA - Translational Brain Medicine, Aachen, Germany
[d] Department of Biomedicine, University of Basel, Basel, Switzerland
[e] Institute of Medical Genetics and Pathology, University Hospital Basel, Basel, Switzerland

ARTICLE INFO

Keywords:
cytoarchitecture
receptor architecture
Julich-Brain atlas
Allen Human Brain Atlas
cortical organization

ABSTRACT

Brain areas show specific cellular, molecular, and gene expression patterns that are linked to function, but their precise relationships are largely unknown. To unravel these structure-function relationships, a combined analysis of 53 neurotransmitter receptor genes, receptor densities of six transmitter systems and cytoarchitectonic data of the auditory, somatosensory, visual, motor systems was conducted. Besides covariation of areal gene expression with receptor density, the study reveals specific gene expression patterns in functional systems, which are most prominent for the inhibitory $GABA_A$ and excitatory glutamatergic NMDA receptors. Furthermore, gene expression-receptor relationships changed in a systematic manner according to information flow from primary to higher associative areas. The findings shed new light on the relationship of anatomical, functional, and molecular and transcriptomic principles of cortical segregation towards a more comprehensive understanding of human brain organization.

1. Introduction

Functional systems such as visual, motor, auditory and somatosensory are part of specific networks that process, integrate, and modify information. Information flow has been described in terms of hierarchical processing, e.g. in the primate visual (Van Essen, Anderson, & Felleman, 1992) and auditory systems (Kaas & Hackett, 2000) . In addition, systematic macroscopic gradients across the entire brain, which are organized along cortical hierarchies have been proposed as being drivers of brain function (Wang, 2020). The hypothesis was formulated that such hierarchies are also reflected in gene expression patterns related to the receptor architecture of brain areas of different brain regions (Burt et al., 2018).

Brain areas have a specific cyto-, receptor- and fiber architecture, individual patterns of immunohistochemistry and gene expression, to list only major properties (Amunts & Zilles, 2015). On top of this, functional systems also show a specific balance of receptor types (Zilles and Palomero-Gallagher, 2017). Studies of motor and sensory cortices have provided evidence that receptor concentrations change in a hierarchical way within functional systems, and areas belonging to the same functional system have a more similar receptor balance than areas belonging to different functional systems (Zilles & Amunts, 2009).

The pattern of changes within functional systems differs between receptor types. Receptors can be classified in dependence on whether signal transduction occurs via ion channels (ionotropic receptors) or G-protein coupled (metabotropic receptors). Ionotropic receptors consist of different subunits, each encoded by a single gene, while metabotropic receptors are monomeric structures and thus encoded by one gene. Ionotropic receptors are composed in a specific combination of receptor subunits, which can undergo changes during development (Bar-Shira, Maor, & Chechik, 2015; Fritschy, Paysan, Enna, & Mohler, 1994; Henson et al., 2008) . A receptor subunit switch changes the properties of the receptor, e.g., conductance, ion block, ligand binding, trafficking, insertion in the plasma membrane and recycling (Farrant & Nusser, 2005; Groc et al., 2006; K. B. Hansen et al., 2018). Such switches are responsible for synaptic plasticity and synaptic strength

* **Corresponding author:** Daniel Zachlod
E-mail address: d.zachlod@fz-juelich.de (D. Zachlod).

https://doi.org/10.1016/j.neuroimage.2022.119286.
Received 17 December 2021; Received in revised form 22 March 2022; Accepted 5 May 2022
Available online 19 May 2022.

(Collingridge, Isaac, & Wang, 2004; Das et al., 1998; Gambrill & Barria, 2011; Lau & Zukin, 2007). A disturbance in the balance of receptors and their subunits is often associated with diseases, e.g., schizophrenia, epilepsy, neuropathic pain, Alzheimer's and Huntington's disease (Baulac et al., 2001; Hashimoto et al., 2008; Hines, Davies, Moss, & Maguire, 2012; Limon, Reyes-Ruiz, & Miledi, 2012; Mahfooz et al., 2016).

The receptor subunit gene expression varied between different rodent brain regions, which seems to be relevant for the functional differentiation of the brain (Hörtnagl et al., 2013; Pirker, Schwarzer, Wieselthaler, Sieghart, & Sperk, 2000; Sieghart & Sperk, 2002; Wisden, Laurie, Monyer, & Seeburg, 1992). Data on the human brain are much sparser and more fragmented. Considering the manifold differences between species in brain structure and function, it is mandatory to extend such studies to the human brain, a prerequisite to also better understand the pathogenesis of brain disorders with alterations in neurotransmitter systems and differences in excitation and inhibition (e.g., (Meunier, Chameau, & Fossier, 2017)).

To disclose the rules along which the different properties of areas change across the cortex, and how their combination contributes to the function of systems or hierarchical position, we have brought together data of two different brain atlases. The Julich-Brain atlas (Amunts, Mohlberg, Bludau, & Zilles, 2020) with its cytoarchitectonically defined brain areas together in combination with receptor data, and the gene expression data from 282 tissue blocks of the Allen Human Brain Atlas (M. J. Hawrylycz et al., 2012). We investigated the relationship between genes and densities of neurotransmitter receptors that are driven by their genes in 15 areas of the visual, auditory, somatosensory and motor systems, analysed the relationship of gene expression data with the concentrations of 12 receptor types for five different neurotransmitters to explore gene transcript-receptor relationships, and addressed differences and similarities between and within the functional systems and their areas (Fig. 1).

2. Materials and Methods

2.1. Quantitative receptor autoradiography

Six hemispheres (4 male, 2 female; age 72-79 years) were used for quantitative in vitro receptor autoradiography (Extended Data table 1). The brains came from the body donor program of the Heinrich Heine University of Düsseldorf. The donors had no history of neurological or psychiatric disease and had given their written consent according the Ethics Committee of the Heinrich-Heine University Düsseldorf. Brains were removed within 16 hours post-mortem. Each hemisphere was divided into 5 to 6 coronal slabs of about 3 cm thickness. Slabs were frozen at -50 ˚C in isopentane and stored at -70 ˚C in airtight bags.

Slabs were serially sectioned (20 μm thickness) at -20 ˚C in a large-scale cryostat microtome. Sections were thaw-mounted onto gelatin covered glass slides and dried overnight before receptor labelling according to previously published protocols (Palomero-Gallagher & Zilles, 2018; Zilles et al., 2002). Adjacent serial sections were used for the demonstration of 12 different receptor binding sites (Extended Data table 2) as well as of cyto- and myeloarchitecture (Palomero-Gallagher & Zilles, 2017; Zilles & Amunts, 2009). Thus, each set of these alternating serial sections provides information on the regional and laminar distribution of 12 different receptors and the cyto- and myeloarchitecture in a small tissue volume. It is immediately followed by the next set of sections treated accordingly throughout the entire hemisphere.

The receptor labelling started with the preincubation (Palomero-Gallagher & Zilles, 2018; Zilles et al., 2002). In this step, the sections were rehydrated, and thereby, all endogenous substances which could block the receptor binding site were washed out. In the main incubation, the sections were exposed to a solution containing a receptor-specific tritium labeled ligand (nM concentration) to measure the total binding. In parallel experiments, non-specific binding was determined in the same solution additionally containing a non-labeled receptor specific ligand (μM concentration) as displacer at the binding site. The specific binding of a ligand is the non-specific binding subtracted from the total binding. As for the here used experimental protocols the non-specific binding was less than 5% in all cases, the total binding is accepted as a good approximation of the specific binding. A rinsing step stopped the incubation procedure and removed the non-bound radioactive ligand and the buffer salts from the sections. The sections were coexposed with plastic scales of known concentrations of radioactivity (Microscales, Amersham) against β-radiation sensitive film (Hyperfilm, Amersham, Braunschweig, Germany) for 4-18 weeks. The autoradiographs and scales were digitized at 8 bit gray-value resolution with an image analysis system (Axiovision, Zeiss Germany). The measurement of the different gray values of the plastic scales and their known radioactivity concentrations resulted in a nonlinear calibration curve, which enabled a linearization of gray values and radioactivity concentrations. Then, these linearized radioactivity concentrations were used to measure receptor concentrations (fmol/mg protein). Additionally, for a better visual demonstration of the various receptor densities, the images were color-coded. For details of experimental and analytical methods see (K. Zilles et al., 2002)(Palomero-Gallagher & Zilles, 2018).

Mean receptor densities were obtained by densitomentric analysis of the autoradiographs. Therefore, areas were identified on autoradiographs and their exact position was checked on neighbouring cell-body stained sections according to previous cytoarchitectonic mapping studies of our own group, summarized in the Julich-Brain (Amunts et al., 2020) (for an overview of analysed areas see Extended Data table 3). Pixel values of linearized autoradiographs were extracted from traverses defined perpendicularly to the cortical ribbon. On this basis, the mean receptor density was calculated (fmol/mg protein) and averaged over three neighbouring sections (Palomero-Gallagher & Zilles, 2018).

Receptor fingerprints plot these grand mean of multiple receptor densities in polar coordinates. Receptors were grouped according to their functional properties from excitatory, inhibitory to modulatory. The shape of the receptor fingerprints indicates the similarity of brain areas concerning the multireceptor expression pattern.

2.2. Julich-Brain Atlas

The Julich-Brain atlas (http://www.jubrain.fz-juelich.de) is part of the HBP Human Brain Atlas (https://www.humanbrainproject.eu/en/explore-the-brain/atlases/), and provides probabilistic maps of cytoarchitectonic areas in stereotaxic space, based on image analysis in a (second) sample of ten post-mortem brains. Brains were obtained from the body donor program of the Heinrich-Heine University Düsseldorf in accordance to legal and ethical requirements. The donors had no history of neurological or psychiatric disease and gave their written consent according the Ethics Committee of the Heinrich-Heine University Düsseldorf. The post-mortem delay did not exceed 24 hours. Brains were fixed in 4% formalin or Bodian, paraffin-embedded, serially sectioned (20µm), and stained for cell bodies (Amunts et al., 2020). Areal borders were identified using image analysis and statistical methods, and mapped to high-resolution scans of these sections (Schleicher, Amunts, Geyer, Morosan, & Zilles, 1999). Sections with the areal borders were 3D reconstructed and transferred to the Julich-Brain Atlas (http://www.jubrain.fz-juelich.de). Maps of somatosensory and motor areas of the Julich-Brain Atlas were used as regions-of-interest for transcriptomic and receptor density analysis (Extended Data, Table 3). Furthermore, for each functional system the maps of its brain areas were combined with the JuGex tool. These merged maps of functional systems were used in JuGex to analyze system-specific gene expression between two functional systems.

Areas of the somatosensory (area1-3 (Geyer, Schleicher, & Zilles, 1999; Grefkes, Geyer, Schormann, Roland, & Zilles, 2001)), visual (areas hOc1-4 (Amunts, Malikovic, Mohlberg, Schormann, & Zilles, 2000; Kujovic et al., 2013; Rottschy et al., 2007)) and auditory (areas Te1,

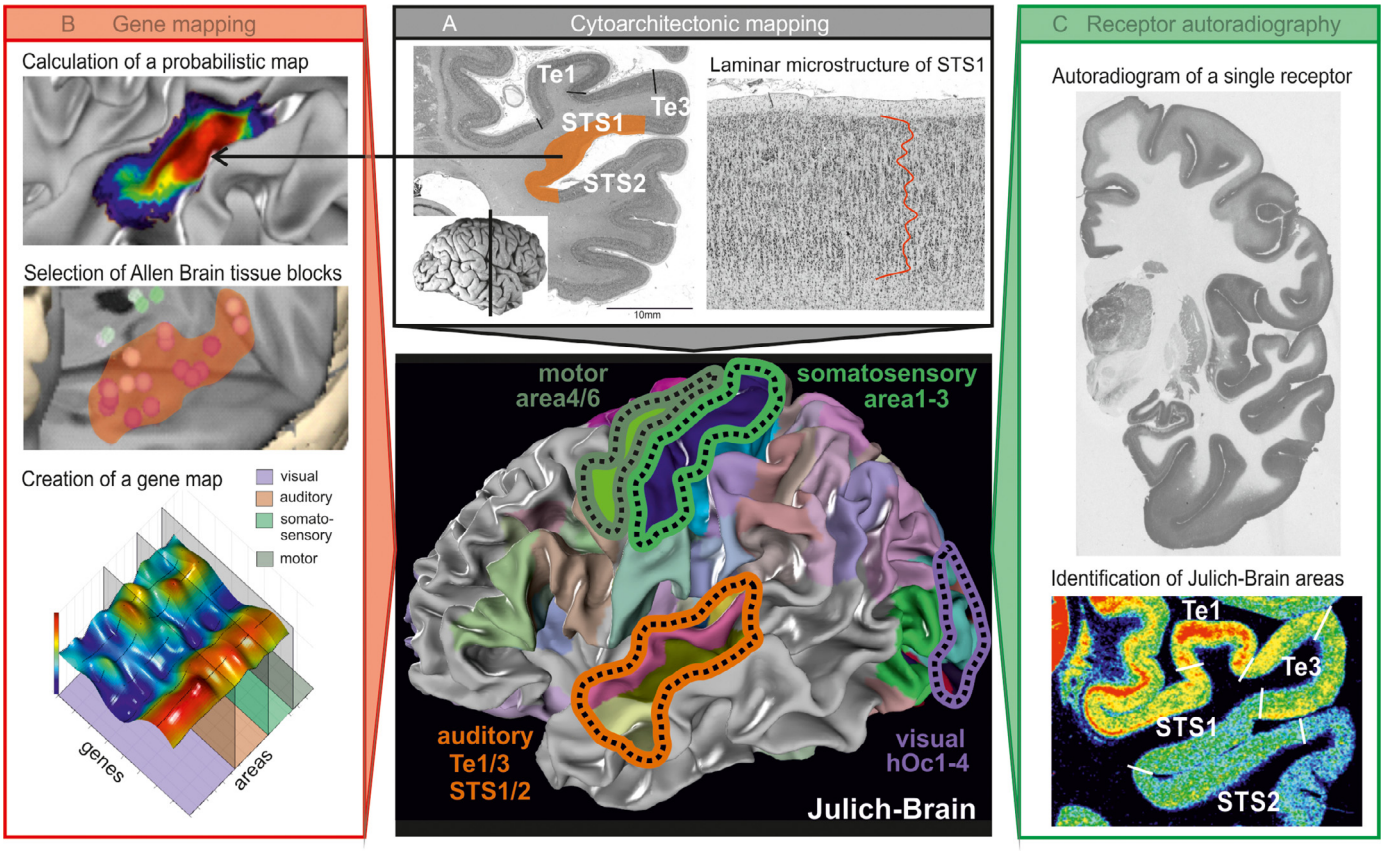

Figure 1. The Julich-Brain Atlas is a tool to integrate receptor and gene expression data.
(A) Area STS1 of the superior temporal sulcus (STS) belongs to the auditory system. It has been mapped in ten post-mortem brains using statistical tools and image analysis (Zachlod et al., 2020) and a probabilistic map has been computed indicating the localization of the area in 3D-space. This map is superimposed with gene expression data from the Allen Human Brain Atlas (B). STS1 has also been identified in receptor-autoradiograms (here the muscarinic M_2 receptor for acetylcholine) of another sample of post-mortem brains; receptor densities are color-coded with red tones showing high concentrations, and blue tones coding for low concentrations (C). Expression of genes coding for receptors subunits was visualized by a surface-based gene map for each receptor type, so that differential gene expression for specific receptor subunits can be compared between functional systems (B). The gene expression was then correlated with the receptor density obtained by quantitative receptor autoradiography for each receptors type.

Te3, STS1, STS2 (Morosan et al., 2001; Morosan, Schleicher, Amunts, & Zilles, 2005; Zachlod et al., 2020)) cortex were compared between each other and with those of the motor cortex (area4 (Geyer et al., 1996), area6 (Amunts et al., 2020)). Subareas were subsumed under the area name to obtain the maximum of tissue blocks for the gene analysis (see next paragraph). That means, area 3 consists of Juelich brain area 3a and 3b, area 4 of 4a and 4p and the premotor area of 6d1, 6d2 and 6d3. For receptor densities taken in subareas 3a and 3b and the dorsal and ventral mean density of area hOc2, the areal mean was used.

2.3. Allen Human Brain Atlas

The Allen Institute for Brain Science provides transcriptome data for genes for the entire human adult brain (M. Hawrylycz et al., 2015; M. J. Hawrylycz et al., 2012). The microarray data for this study are derived from the Allen Human Brain Atlas (http://www.human.brain-map.org), which comprises over 62000 gene probes per profile collected in about 500 samples per hemisphere in six donor brains (M. Hawrylycz et al., 2015; M. J. Hawrylycz et al., 2012). For detailed information please consult the white papers (http://help.brain-map.org/display/humanbrain/Documentation). Gene expression in the tissue blocks was normalized over the whole brain and the results in z-scores were mapped on a 3D anatomical space (icbm152). Tissue blocks were addressed with a macroanatomical label. Gene expression data was publicly available and was used in this study to investigate areal gene expression.

2.4. Gene expression in brain areas

A gene list was created using PubMed to search for receptor genes in the human brain with the receptor name as entry. The list comprises 53 genes of metabotropic and ionotropic receptors or their subunits from all transmitter systems (Extended Data table 4). With the JuGEx Toolbox (available at http://www.fz-juelich.de/inm/inm-1/jugex), the gene names of the list were converted into a format of the Allen Human Brain microarray dataset (http://www.human.brain-map.org), so that the gene expression of a tissue block can be accessed by the Allen Human Brain probe-ID.

For this study, we examined 15 cytoarchitectonically defined sensory and motor areas of the Julich-Brain atlas (Amunts et al., 2020). The atlas provides maps in icbm152 and Colin27 reference space. So, the maps in icbm152 reference space could directly be used for transcriptome analysis of the Allen Human Brain microarray dataset, which is provided in the same reference space. The extension of areas was limited to 60% of the original size (80% for Te1 to maximize the number of tissue blocks; in this case the position of tissue blocks was visually checked) to avoid false positive results. The JuGEx toolbox was used to extract transcriptome data from the Allen Human Brain microarray database for both hemispheres of the six available brains. All tissue blocks of an area (Extended Data table 5) were pooled before the median receptor gene expression for each area was calculated.

2.5. Gene expression in functional systems

Differences in receptor gene expression between functional system (Supplement Table S1) were analysed by merging the Julich-Brain areas of each functional system. These newly created maps are representing the surface of the functional system as defined in this study and were used in JuGEx with a threshold of 20 % to search for differential receptor gene expression. First, the tissue blocks within a functional system were selected. Then differential expression of 53 receptor genes (Extended data, Table 4) were analysed between two functional systems and the results were statistically tested with the JuGex pipeline with a permutated ANOVA (permutation rate: 10000) and FWE corrected.

2.6. Analysis of areal gene expression

Median gene expression data of all receptors were plotted in polar coordinates per area. This plot was called a “genetic fingerprint” in analogy to “receptor fingerprints” (see above). It characterizes the areal gene expression pattern and enables a comparison between areas and regions. These datasets were analyzed with a multivariate statistical approach, and the result depicted as an MDS plot. For ionotropic receptors, the transcriptome data was depicted in a surface plot using Matlab. This visualization enables the researcher to analyse the genetic data in an easy and intuitive way and shows clearly the differential gene expression between regions. For 12 receptor types, the median gene expression of an area was compared to its mean receptor density (Extended Data Table 6). For ionotropic receptors the mean receptor density was compared to the gene of the major isoform. The two datasets were compared with Pearson correlation and statistically tested with two-sample t-test and corrected for multiple comparisons (Benjamini-Hochberg FDR correction). To analyse co-expression of receptor genes, 26 gene pairs were analyzed for the 15 brain areas with Pearson correlation, statistically tested with two-sample t-test and FDR corrected for multiple comparisons (Extended Data Table 7).

3. Results

3.1. Comparison of functional systems

The similarity and dissimilarity of 15 areas of four different functional systems based on their gene expression was captured by Multidimensional scaling (MDS) (Fig. 2). MDS depicts the distances of the analysed areas regarding the gene expression pattern of 53 receptor genes (listed in Extended data Table 4), and projects it to a two-dimensional surface. It reveals that the areas differ with respect to their gene expression pattern. Areas tend to cluster within functional systems (Fig. 2).

Somatosensory areas (green) clustered separately from those of the auditory system (orange), but both were more similar to each other than to the areas of the visual system (purple). Most of the areas of the visual system were most dissimilar from the rest of the areas in receptor gene expression, except area hOc4v, a higher visual area of the ventral stream that clustered close to those of motor and somatosensory areas. This gradient within the visual system is shown in Figure 2A.

For comparison with their protein level, the areas were grouped according to their mean receptor density as obtained from autoradiograms of multiple receptor binding sites of six hemispheres (Fig. 2B). Areas also form clusters, and the four functional systems can be distinguished from each other. For example, the visual system gives a cluster that is seprate from the other three.

The comparison of the two MDS plots shows that all four functional systems form clusters for both the receptor density and the receptor gene expression. In addition, gradients can be identified within a functional system (e.g., see grey lines in Fig. 2A).

While MDS combines single values of gene expression (and receptor densities) to provide an overall distance measure for similarties and dissimilarties between areas and systems, gene expression fingerprints (genetic fingerprints) and receptor fingerprints disclose the balance of individual levels in each area, and capture area-differences by different shapes (K Zilles et al., 2002) (Fig. 3 and Supplement Fig. S2).

The receptor fingerprints integrate mean densities of 12 receptor binding sites; their shape differs between the auditory and visual systems (Fig. 3A; Supplement Fig. S2 for the other two systems). The visual system has higher mean receptor densities of NMDA and $GABA_A$ receptors, but lower values for the M_3 receptor than the auditory system (Fig. 3A). These prominent differences for the ionotropic excitatory NMDA receptor and the inhibitory $GABA_A$ receptor can also be found in the genetic fingerprint. However, the auditory system depends on a different subset of receptor genes and shows higher values than in the visual system for excitatory NMDA and inhibitory GABAA receptor genes (asterisks in Fig. 3B).

Areas of the visual system are dominated by high peaks in a few receptor genes (GRIN2A, GABRA1, GABRA4, GABRB2, GABRG2), mainly those coding for subunits of a ubiquitous receptor form, called major isoform, whereas areas of the auditory system have differential receptor gene expression. Comparison of the auditory and visual systems shows that 56 % of the glutamatergic and 70 % of the GABAergic receptor genes are differentially expressed between both systems. These genes are GRIN2A, GRIN2B and GRIN3A for the NMDA receptor and nearly all pore forming subunit genes of the $GABA_A$ receptor (for details see Supplement Table S1). In total, 62 % of all analysed genes are differentially expressed. Receptor genes GRIN3A (NMDA), GABRA1/5, GABRB1, GABRD (GABA) and the gene of the serotonin 5-HT_{1A} receptor are differentially expressed between the auditory and the visual system, but not when comparing the somatosensory and motor systems.

Comparing the somatosensory and motor systems, the value of significantly regulated genes dropped to 17 %. Only 17 % of the glutamatergig (i.e. GRIK2,4, GRIN2A) and GABAergic (i.e. GABRA2-4, GABRG1) genes are differentially expressed (Supplement Table S1). The genetic similarity of the somatosensory and motor systems is greater than in corresponding receptor fingerprints. The somatosensory system shows an overall higher receptor density than the motor system. Comparing the grand mean between the functional systems the receptor densities of kainate, M_1, α_2, 5-HT_{1A} and D_1 receptors more than doubled in the somatosensory system (Supplement Fig. S1).

When looking to the areas within the functional systems, it can be seen that the primary auditory area (Te1) differed from higher associative areas of the auditory cortex (Te3, STS1, STS2) in 17 % of all analysed receptor genes of the glutamatergic, GABAergic, cholinergic and serotoninergic transmitter systems (genes listed in Supplement Table S2). Prominent examples of different gene expression in the primary auditory area were found for the GABAergic, cholinergic and serotoninergic systems and are highlighted with an arrow head in Fig. 3B. Genes of the primary and higher visual areas did not pass the treshold ($p > 0.05$).

3.2. Analysis of metabotropic receptors

Metabotropic receptors revealed a system- and area-specific gene expression pattern. For example, the density of the muscarinic acetylcholine M_2 receptor was correlated with its receptor gene expression in all areas of the three sensory systems (Fig. 4A).

The M_2 receptor gene showed a high expression in primary sensory areas hOc1, Te1, and area3. The gene expression decreased in secondary sensory areas and is lowest in higher associative areas. Such decrease from primary to higher associateive areas was also found in the areal receptor densities of the different functional systems (Fig. 4B). In the autoradiograms, all primary sensory areas hOc1, Te1 and area3 show prominent high receptor densities as compared to the primary motor cortex, which has low densities.

Figure 4A showed that for the metabotropic M_2 receptor the RNA levels correspond to their receptor density pattern. Other gene - receptor density correlations are shown in Supplement Fig. S13-15. Metabotropic

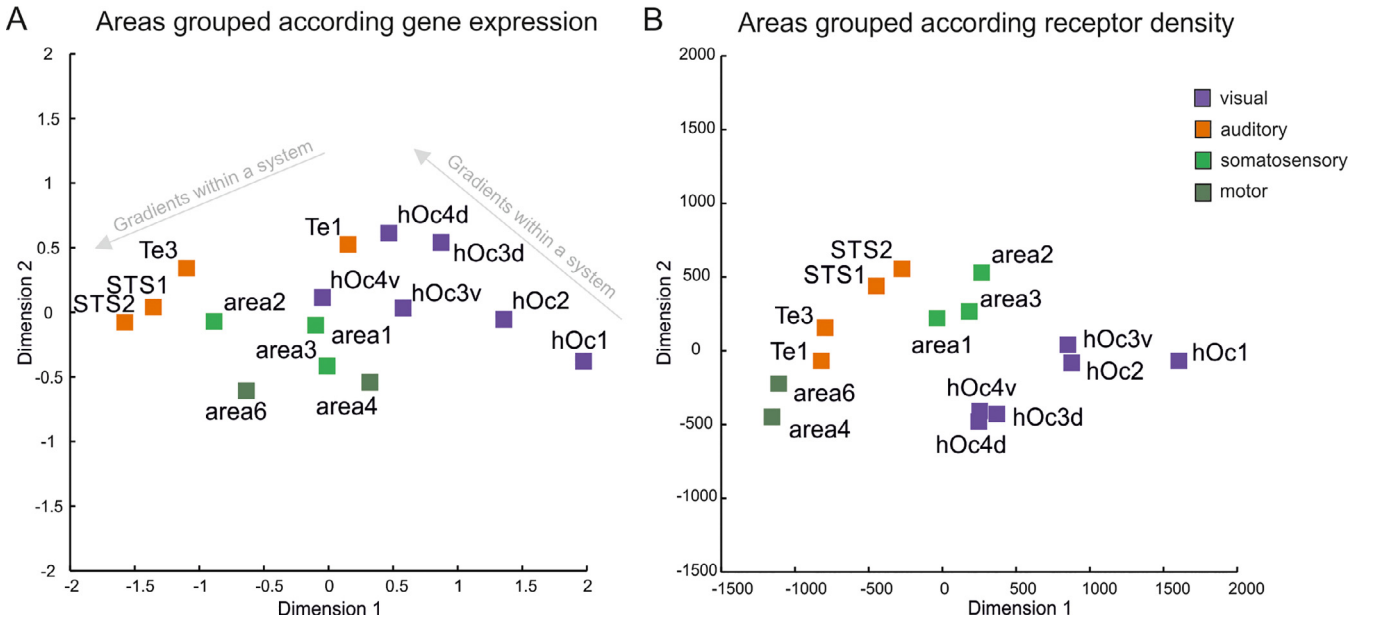

Figure 2. Multidimensional scaling for receptor gene expression and mean receptor density.
Functional systems cluster separately both in receptor gene expression (A) and mean receptor density (B) for auditory (orange), visual (purple), somatosensory (green) and motor (olive) systems. Areas of a functional system can be characterized in both modalities and showed a gradient from primary to higher associative areas (here shown for the gene expression of the visual and auditory systems in A). The unique receptor gene expression pattern, i.e., the receptor gene expression of 53 receptor genes in a brain area, characterizes the position of an area in a functional hierarchy. The same is true for the receptor pattern, which also enables to identify clusters (B).

receptors are encoded by one gene per receptor, whereas ionotropic receptors have a more complex structure. They consist of different subunits encoded by multiple genes. The different receptor genes, which are needed to form a functional receptor, require a different analysis for the ionotropic receptors.

3.3. Analysis of ionotropic receptors

In contrast to metabotropic receptors, each ionotropic receptor is encoded by several subunit genes. The combination of receptor subunits results in different isoforms, but the receptor subunit composition is not known for all of them. Therefore, biochemical and physiological data is often obtained with the most abundant receptor isoform, called major isoform. The excitatory NMDA and inhibitory $GABA_A$ receptors showed large differences in the receptor subunit gene expression between the functional systems in the genetic fingerprints (Fig. 2). These two receptors were investigated in more detail.

3.4. Analysis of the inhibitory $GABA_A$ receptor

The $GABA_A$ subunit gene expression differed between the four functional systems (Fig. 5A). The comparison of the primary areas revealed that the gene expression pattern of primary auditory and somatosensory areas differed in the expression of many genes from that of the primary visual area (Fig S3 A+B). The primary somatosensory area showed smaller differences to the primary auditory area (Fig S3 C) than to the primary visual area. Interestingly, the lowest difference was found between primary somatosensory to primary motor area 4 (Supplement, Fig. S4 D).

To analyze the manifold relationships between gene expression, functional systems and hierarchical position of an area within its functional system in an intuitive and comprehensive way, a surface-based gene plot was generated. This plot encompasses receptor subunit gene expressions for all areas (Fig. 5A). The surface plot of the $GABA_A$ receptor demonstrates, that each sensory system has its own subset of characteristic, highly expressed receptor subunit genes. For example, the visual areas have a common receptor gene expression pattern, which is dominated by high RNA levels from few receptor subunit genes such as GABRA1, GABRB2 and GABRG2. In addition, subunit genes are differentially expressed within a functional system, but these differences are rather minor as compared to the differences between the subunit genes within a system (Fig. 5A).

Gene expression increases for several receptor subunits when moving in the graph from the visual to the auditory system. These receptor subunit genes include GABRA3, GABRA5, GABRB1 and GABRB3; they have relatively low levels in the visual system (blue and green “valleys”).

The expressions of all subunit genes of the major isoforms, which are GABRA1, GABRB2 and GABRG2, correlated strongly (r=0.79 to 0.86; Fig. 4 B). GABRD codes for the δ-subunit and replaces the γ-subunit in the functional receptor. The expression of GABRD correlated with the GABRA1 subunit gene of the major isoform, and is not regionally overexpressed (Supplement, Fig. S3). But two other pairs of subunit genes seem to be coupled and are upregulated only in the auditory system. The genes GABRA3 and GABRB1 were expressed at the same level throughout all analysed areas ($r > 0.92$) and showed the opposite expression pattern to that of the major isoform (Fig. S7; negative correlation of the subunit genes to GABRA1/GABRB2: $r < -0.88$). Differential gene expression was also found for the gene pair GABRA5 and GABRB3. Both genes correlated highly (r=0.90) and are prominently upregulated in the auditory areas (Fig. 5C). As a common feature, the two pairs show a low to average expression in the visual areas, whereas they are upregulated in the auditory areas (highlighted with an orange rectangle; see Fig. 5C and Fig. S7).

3.5. Analysis of the excitatory NMDA receptor

Regional differences in expression levels of receptor subunits for the ionotropic NMDA receptor for glutamate were found as well. The gene map of the NMDA receptor showed high expression levels of subunit genes forming the major isoform (GRIN1 and GRIN2A) throughout all analysed areas (Supplement, Fig. S8) with a maximum in the visual system. The gene expression and receptor density levels of GRIN2A corre-

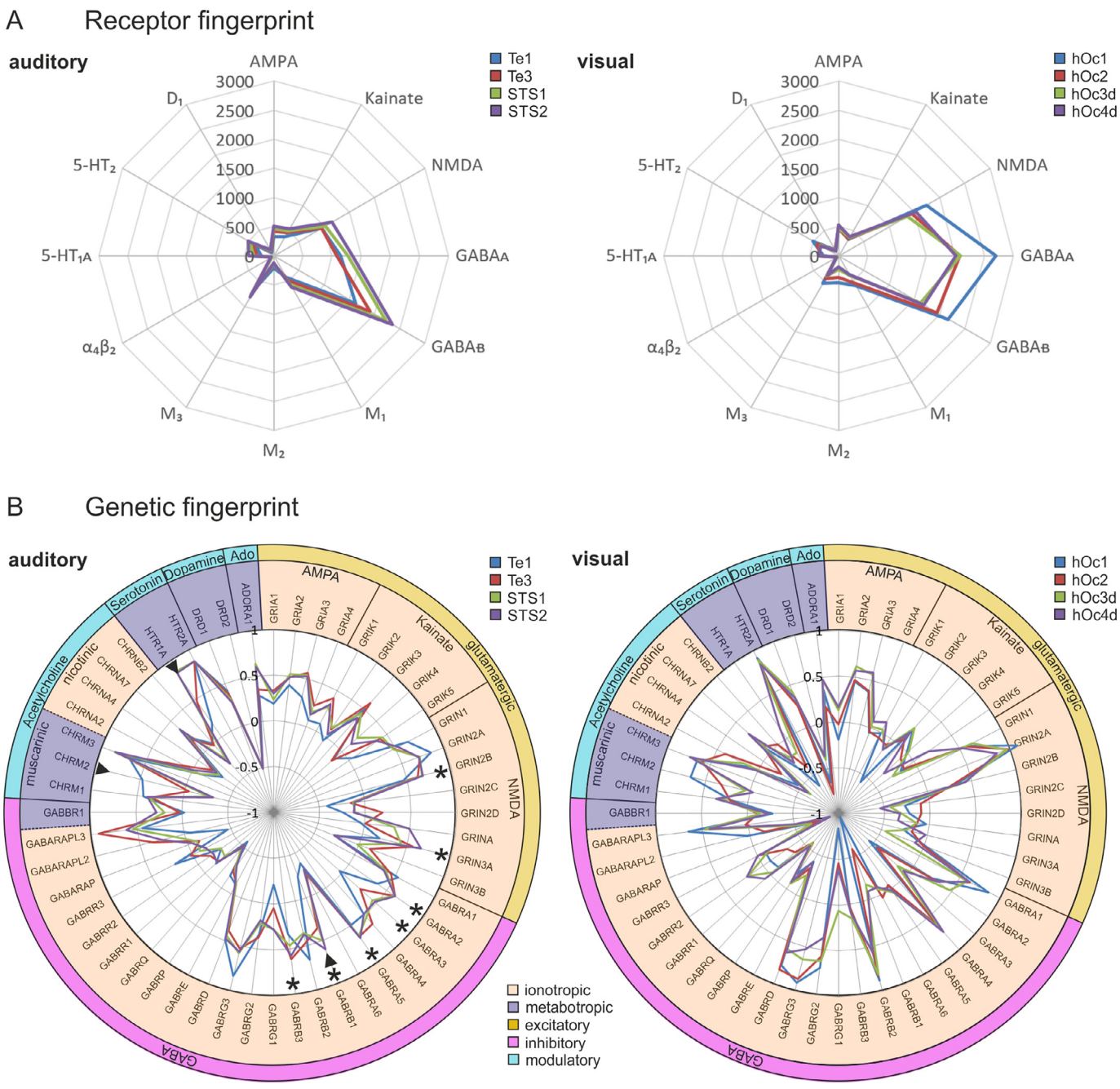

Figure 3. Receptor and genetic fingerprints of visual and auditory areas

Receptor fingerprints show the balance of mean receptor densities in a brain area, and differ between the areas of the auditory and visual systems as indicated by the different shapes of the fingerprints (A). Differences between both systems were also pronounced for genetic fingerprints (B). The receptor types are color-coded to label ionotropic (in pale orange) vs. metabotropic (purple; inner ring), and different types of excitatory (ocker), inhibitory (light blue) and modulatory (pink, outer ring). Gene expression fingerprints of 53 receptor genes in auditory (Te1,3, STS1,2) and visual areas (hOc1,2,3d,4d); coloured lines represent gene expression levels per area. Receptor genes were grouped from glutamatergic (AMPA, kainate, NMDA), GABAergic ($GABA_A$) which are ionotropic receptors, to the metabotropic muscarinic cholinergic ($M_{1\text{-}3}$), ionotropic nicotinic cholinergic, metabotropic serotoninergic ($5\text{-}HT_1$, $5\text{-}HT_2$) and dopaminergic receptors (D_1). The order of the receptor genes in the gene expression fingerprint reflects the functional receptor category from excitatory (glutamate), to inhibitory (GABA) and modulatory (acetylcholine, serotonin, dopamine, adenosisn). The scaling is identical in each case. Receptor gene expression within areas of a functional system are more similar to each other than between systems. The primary auditory area differed in M_2, $GABA_A$ and $5\text{-}HT_{1A}$ receptor genes from the associative areas (arrow heads). Note large differences between the two systems of the ionotropic $GABA_A$ and NMDA receptors with higher levels in the auditory areas than in the visual areas for several receptor subunit genes (asterisks). Ado – adenosine.

lated for all studied areas (Supplement figure S8). In the visual system no other subunit gene showed higher expression levels. However, a different subunit gene expression was found for auditory and somatosensory areas. A comparison of primary auditory (Te1) and primary visual (hOc1) areas revealed that the GRIN3A gene is more highly expressed in area Te1 (Supplement, Fig. S10). Comparing all analysed areas, we found that GRIN3A has high expression levels throughout auditory areas (orange rectangle in Supplement, Fig. S11), whereas in somatosensory areas the gene expression is average and in the visual system slightly below brain average. The regulatory NMDA gene GRINA was found to

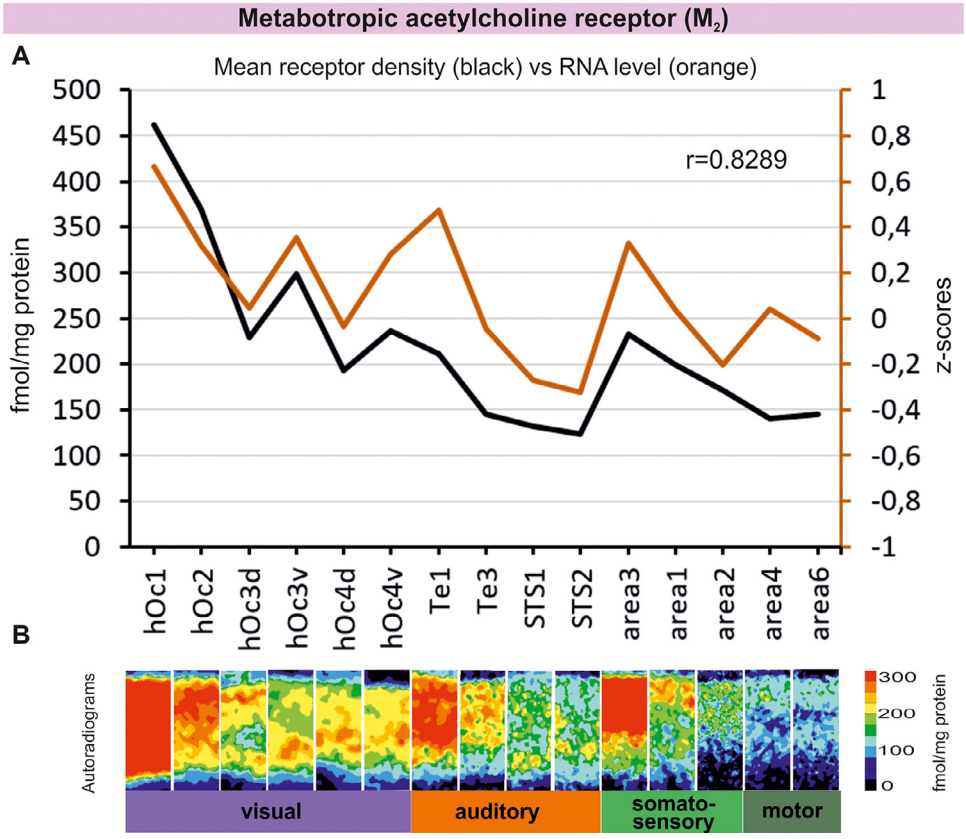

Figure 4. Area-specific patterns of the metabotropic M_2 receptor: receptor density (left y-axis) and gene expression (z-scores, right y-axis)
The receptor density (black curve) of the 15 areas co-varies with the expression of the metabotropic M_2 receptor gene (orange curve; 3A). Autoradiograms for each area are shown in 3B. Note the high concentrations of the receptor in primary areas (leftmost in each functional system), which is in accordance with previous findings on a high M_2 receptor concentration (Zilles and Palomero-Gallagher, 2017). The concentration decreases from left to right within systems, towards higher areas.

be highest in the somatosensory areas (Supplement, Fig. S12). We found that two NMDA subunits, GRIN2C and GRIN2D, were expressed below average. GRIN2C is only expressed in the cerebellum, and GRIN2D during development. The low expression rates of these genes found in all analysed areas strengthen the areal gene expression gradients proposed in this study.

4. Discussion

The present study targeted three levels of cortical organization: cytoarchitecture, neurotransmitter receptor architecture and neurotransmitter receptor gene expression. It elucidates principles of human brain organization for different functional systems, going beyond the simplified view of a “mosaic” of areas forming the neocortex. The present study reveals relationships between gene expression patterns and the receptor types for which they code. It suggests that the expression of receptor genes depends on the position of the brain area within a functional system. On a more abstract level, areas can be conceptualized in terms of (nested) hierarchies and gradients. Hierarchical concepts of brain organisation were introduced for cytoarchitecture (Zilles & Amunts, 2012), connectivity (Goulas, Zilles, & Hilgetag, 2018) and molecular architecture (Zilles and Palomero-Gallagher, 2017). A recent study (Goulas et al., 2021) showed that the diversity of receptor densities changes from cytoarchitectonically defined sensory to association areas forming a natural axis for brain hierarchy. Along this axis the ratio between the excitatory and inhibitory receptor densities increases, as well as the densities of metabotropic receptors.

The patterns of cytoarchitecture, receptor architectonics, gene expression and connectivity, changes when moving from one to the neighbouring area (Amunts & Zilles, 2015). This finding alone would be sufficient to explain cortical segregation in terms of a mosaic of areas, but does not explain their specific role in networks underlying a certain cognitive function. To disclose the rules by which the aspects of brain organisation are linked to each other, and what the differences between areas are depending on their role in a certain functional system is a topic of intensiv research, and contributes to reveal the nature of cortical segregation and intrinsic organization.

A multi-modal approach was employed in the present study to address this topic, targeting a large number of receptor types of different neurotransmitters and related genes. The term hierarchy in the present study refers to systematic changes within a functional system, i.e., from primary to higher associative areas, and applies to the visual, auditory, somatosensory and motor systems, each represented by several cytoarchitectonically identified areas.

The analyses showed correlations between gene expression and receptors, not only for metabotropic, but also several ionotropic receptor types. This is interesting, considering the fact that on a global level (44 brain areas across the cortex) gene expression data of the Allen Brain Institute does not seem to be a good predictor for receptor density (J. Y. Hansen et al., 2021). The present study revealed that several receptor densities and gene expression covaried in four functional systems. Different from the study by Hansen and colleagues, the present study focused on primary and adjacent areas. We found covariations for muscarinic M_2 receptor, which shows the highest densities in the primary sensory areas (Zilles et al., 2004; Karl Zilles, Axel Schleicher, Nicola Palomero-Gallagher, & Katrin Amunts, 2002), and for GABAA and GABRB2 and NMDA and GRIN2A. Based on the findings of the two studies, it could be hypothesized that covariation would be weaker or non-existing for higher associative areas, a topic for future research.

In addition, differences in the gene expression and receptor patterns between the functional systems in the human brain were demonstrated – first, between sensory and motor systems which has been expected considering the quite distinct role of the motor system as a major output region from that of sensory systems receiving and further processing input. Secondly, differences were found also within sensory systems with the visual system having a unique position. Again, this seems to be plau-

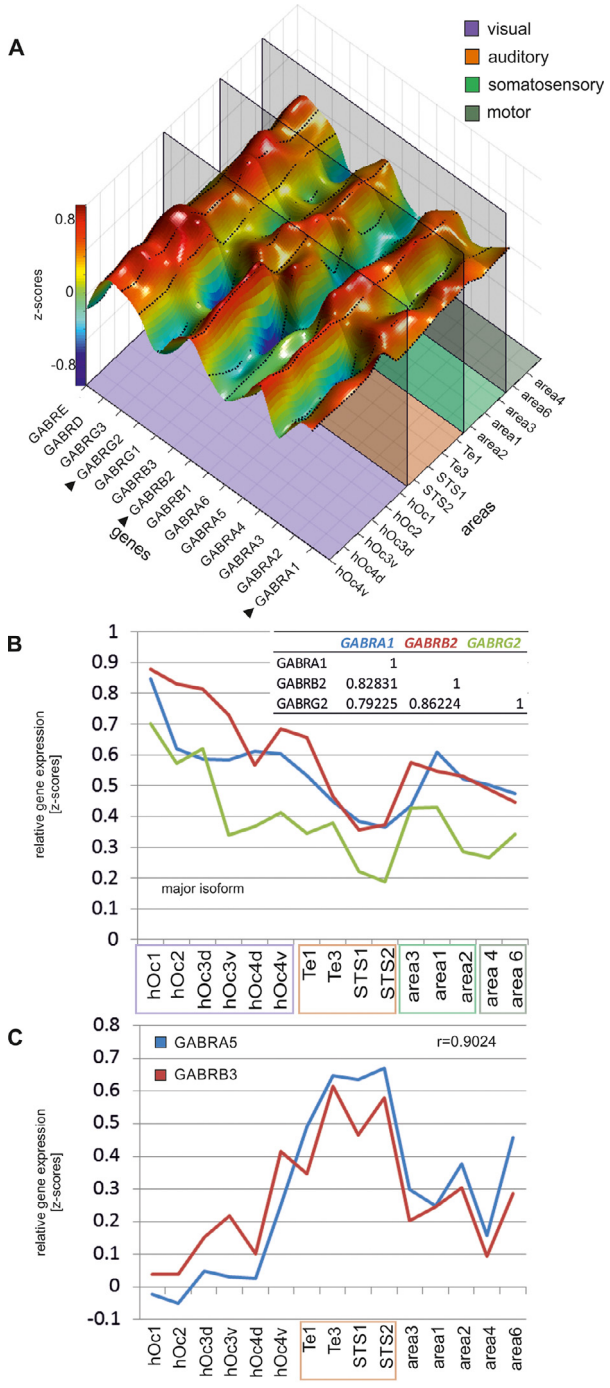

Figure 5. Differential gene expression for $GABA_A$ receptor and receptor densities

The four functional system are characterized by a unique $GABA_A$ receptor subunit gene expression. The visual system (purple) shows high levels in only a few receptor genes (e.g., GABRA1, GABRB2 and GABRG2 coding for subunits of the major isoform, arrow heads), whereas gene expression in the auditory system (orange) is high in other and more receptor subunit genes ("broader peaks" caused mainly by GABRA2, GABRA5, GABRB1 and GABRB3). The motor system shows lower peaks for a few genes (oliv), similar to the somatosensory system (green, A). The $GABA_A$ subunit gene expression of the major isoform GABRA1, GABRB2 and GABRG2 is highest in the visual system. There is an overall high correlation for all areas ($r > 0.79$; B). Other subunit genes, here GABRA5 and GABRB3, are highly expressed in auditory areas (orange box). The overall correlation of GABRA5 and GABRB3 is high, and may contribute to the specifity of the auditory system (C).

sible considering that the visual system has a unique position among the sensory system with more neurons in-between the sensory neuron (rods and cones) and the primary cortex.

Interestingly, the expression of receptor genes depends on the hierarchical position of the brain area within a functional system. This is in line with gene expression gradients reported for visual occipito-temporal areas (Gomez, Zhen, & Weiner, 2019). In the genetic fingerprints, each sensory system showed a region- and area-specific gene expression, which results in their segregation or clustering, respectively, as revealed by multidimensional scaling: within a functional system, the primary areas showed stronger differences in their gene expression than higher associative areas. Such hierarchy was underpinned by receptor density studies (Nørgaard et al., 2021; Zilles and Palomero-Gallagher, 2017).

That brain regions differ in their transcriptome is well-known from animal studies. For example, a system-specific dispersion of cell types was reported by single-cell transcriptomic studies in rodents (Economo et al., 2018; Tasic et al., 2018; Zeisel et al., 2015). Differential $GABA_A$ subunit gene expression was shown in hybridisation studies in rodent brain regions (Sieghart & Sperk, 2002). The present data allow to move one step further, and demonstrate that the human sensory systems are not only specified by their receptor density (Zilles and Palomero-Gallagher, 2017; Zilles et al., 2017), but by an area-specific expression of their receptor (subunit) genes. Metabotropic receptor densities covaried with the receptor gene expression. Exemplarily shown for the M_2 receptor, which has the highest densities in primary areas of sensory systems.

A surface-based gene map was computed for the ionotropic receptors to visualise differential gene expression, which was then further analysed. Interestingly, a different subset of $GABA_A$ receptor subunits was expressed in the auditory compared to the visual system. Correlation analysis of $GABA_A$ subunit genes revealed gene pairs which covaried over all analysed areas and reached its maximum in the auditory system. A coupling of subunit genes was also found in a recent study analyzing the $GABA_A$ expression with the Allen Human Brain labels (Sequeira, Shen, Gottlieb, & Limon, 2019). In this study, genes were correlated in two datasets, the AHBA microarray dataset and the mRNA-Seq dataset of the ADTBI study. The findings of Sequiera et al. in the microarray dataset correspond to those of our study. However, there are also some differences including the factors aging, dementia and TBI. Based on RNA sequencing (ADTBI dataset), the study reported correlations, e.g. for α_2,γ_1 vs γ_2. This was also a finding of the present study, but it did not pass FDR correction. An important difference is related to the underlying brain atlas and parcellation scheme. The present study is based on cytoarchitectonically defined areas of the Julich-Brain atlas, which provide a biological correlate of functional differences between brain areas. However, areas do not necessarily respect anatomical landmarks, and their borders do not coincide with sulcal or gyral pattern in many brain regions (Amunts & Zilles, 2015). Thus, cytoarchitectonic probabilistic maps are expected to be more sensitive and to reveal additional information for those areas in particular, where the relationship between areal borders and sulci is week, e.g. higher associative areas. This allowed to disclose in the present study new correlations e.g. positive correlations of β_2, γ_2, α_1 with the δ- subunit and positive correlations of the α_3- and β1-subunit which are negative correlated to the major isoform and mainly expressed in the auditory system (Fig. S7).

Tight coupling of subunit genes provides strong evidence for the areal receptor composition. There is one small limitation – the absolute concentration of m-RNA is not known due to the normalization procedure in the Allen Human Brain Atlas. It is well accepted, however, that variations in the subunit composition of a receptor change the physiological properties of the receptor, i.e. conductivity, ligand binding, receptor trafficking and recycling (Farrant & Nusser, 2005; Groc et al., 2006; K. B. Hansen et al., 2018) and may therefore specify the areas of a sensory system besides the receptor density (Zilles and Palomero-Gallagher, 2017). It was found that the major isoform correlated with

the receptor density and other isoforms showed a system-specific regulation. In the auditory system the NMDA subunit gene GRIN3A was upregulated. This subunit is known to prevent spiking and is associated with synaptic loss during development (Perez-Otano, Larsen, & Wesseling, 2016; Roberts et al., 2009), but may have a function in the auditory system at concentrations which are 5-fold lower than postnatal (Henson et al., 2008).

The multimodal approach of the present study enables to characterize a brain area by the gene expression fingerprint and unravel its differential gene expression for ionotropic receptors. This areal receptor gene expression could be related to its functional system, despite the methodological and interindividual variability of different modalities. Although there are many regulatory steps from the receptor m-RNA to a functional synaptic receptor (splicing, translation, post-translational modification, folding, assembly, trafficking and integration in the plasma membrane), the transcriptomic data strongly correlated with values from quantitative autoradiography of the corresponding receptors. The tight coupling of receptor subunit genes across brain areas and the upregulation in different functional systems argues for a functional adaption of receptor complexes. These structural receptor changes influence the physiological properties and might specify brain areas besides receptor density.

This study showed a remarkable correlation between gene expression pattern, cyto- and receptor architecture. It must be mentioned, however, that receptor genes (although important for signal transduction and therefore of high functional relevance) represent only one category of genes that contribute to the specifity of a brain area. 85% of the human genes are expressed in at least one brain area with potential functional regulatory mechanisms for the brain area (M. J. Hawrylycz et al., 2012; Negi & Guda, 2017). Here we demonstrated a method to unravel the influence of gene expression pattern on a cytoarchitectonic brain area and relate the results to the functional system of which the brain area is part.

In conclusion, the receptor gene expression is correlated with receptor density as obtained from autoradiograms. These gene expression patterns are specific for the functional systems addressed in the present study, and they change within a functional system along a functional hierarchy, i.e. from primary to higher associative areas. For ionotropic receptors the major isoform correlated with the receptor density. A subset of receptor subunit genes is differentially expressed in different functional systems. E.g. in the visual system only $GABA_A$ subunit genes of the major isoform are upregulated, whereas in the auditory system other receptor subunits seem to play a more important role. We hypothesize that this exchange in receptor subunits contributes to the specificity of the functional system besides the areal receptor density. For the sensory and motor systems of this study a differential receptor gene expression can be observed. We hypothesize that a hierarchical receptor gene expression is also characteristic of other functional systems, including association areas and subcortical nuclei.

Besides regional differences of receptor densities, the analysis of the receptor balance is relevant for studying the healthy brain, and brain of patients (Palomero-Gallagher et al., 2012), chemical neuromodulation and drug efficiency (Cools, 2019). Positron Emission Tomography (PET) allows to study the living human brain, and whole brain maps of the serotonergic, GABA-ergic and domanigergic transmitter systems have been provided in the past few years (Beliveau et al., 2017; Cools, 2019; Nørgaard et al., 2021). Moreover, the mRNA expression for individual subunits in the GABAA and benzodiazepine receptor density have been provided (Nørgaard et al., 2021). The current approach supplements in vivo imaging approaches based on PET, and allows to reach a high spatial resolution, down to the laminar level. Capturing variations of receptor concentrations within the cortical cross section is relevant for the connectivity of an area, and consequently relevant for brain function. In addition, it allows to compare different receptor types, and to study their balance, which is key to achieve a deeper understanding of pathomechanisms, e.g., in epilepsy, but also pain perception (Luo, Kusay, Jiang, Chebib, & Balle, 2021), but not possible in the living human brain. Receptor maps are the basis for predictions of in-vivo PET studies therefore this data has a high synergistic potential. The cytoarchitectonic and receptorarchitectonic data are available in the Julich-Brain and accessible via Ebrains (https://kg.ebrains.eu).

Acknowledgments

We thank Karl Zilles for intensive discussions, and for his contribution to the analysis. His development in the field of receptor autoradiography laid an important foundation for this study.

All brains were obtained through the body donor program of the Department of anatomy at the University of Düsseldorf in accordance to the rules of the local ethics committee (# 4863).

We thank the Allan Brain Institute for providing the gene expression data as a resource open to the community.

This project has received funding from the European Union's Horizon 2020 Framework Programme for Research and Innovation under the Specific Grant Agreement No. 945539 (Human Brain Project SGA3).

Author Contributions

KA developed the study design, supervised the acquisition of brains and their processing, and contributed to the analysis; DZ conducted the study and analyzed the results; SB wrote the JuGEx code and contributed to the analysis; SC contributed to the analysis; NPG co-supervised processing of the brains, co-designed the procedure for quantification of receptor autoradiographs, supervised and contributed to the acquisition of receptor autoradiography data. All authors contributed to the writing of the manuscript and approved publication.

Code availability

We did not use any specific code for this study. Gene-gene and gene-receptor data were analyzed with Pearson correlation, statistically tested with a two-sample t-test and FDR corrected. All analysis were performed with Excel tools. Differential gene expression between areas were performed with JuGex (Bludau et al. 2018; publicly available https://ebrains.eu/service/jugex/). Results were tested with ANOVA and FWE corrected during the JuGex workflow.

Data availability

The JuGEx Toolbox is available at http://www.fz-juelich.de/inm/inm-1/jugex.

The Allen Human Brain microarray dataset is available at http://www.human.brain-map.org.

The Julich-Brain Atlas is available at http://www.jubrain.fz-juelich.de.

Detailed information on cytoarchitectonic areas is stored in the ebrains knowledge graph (https://kg.ebrains.eu)

Competing Interest Statement

none declared

Supplementary materials

Supplementary material associated with this article can be found, in the online version, at doi:10.1016/j.neuroimage.2022.119286.

References

Amunts, K., Malikovic, A., Mohlberg, H., Schormann, T., Zilles, K., 2000. Brodmann's areas 17 and 18 brought into stereotaxic space—where and how variable? Neuroimage 11 (1), 66–84.

Amunts, K., Mohlberg, H., Bludau, S., Zilles, K., 2020. Julich-Brain: A 3D probabilistic atlas of the human brain's cytoarchitecture. Science 369 (6506), 988–992.

Amunts, K., Zilles, K., 2015. Architectonic mapping of the human brain beyond Brodmann. Neuron 88 (6), 1086–1107.

Bar-Shira, O., Maor, R., Chechik, G., 2015. Gene expression switching of receptor subunits in human brain development. PLoS computational biology 11 (12), e1004559.

Baulac, S., Huberfeld, G., Gourfinkel-An, I., Mitropoulou, G., Beranger, A., Prud'homme, J.-F., LeGuern, E., 2001. First genetic evidence of GABA A receptor dysfunction in epilepsy: a mutation in the γ2-subunit gene. Nature genetics 28 (1), 46.

Beliveau, V., Ganz, M., Feng, L., Ozenne, B., Højgaard, L., Fisher, P.M., Knudsen, G.M., 2017. A High-Resolution In Vivo Atlas of the Human Brain's Serotonin System. Journal of Neuroscience 37 (1), 120–128. doi:10.1523/jneurosci.2830-16.2016.

Burt, J.B., Demirtaş, M., Eckner, W.J., Navejar, N.M., Ji, J.L., Martin, W.J., Murray, J.D., 2018. Hierarchy of transcriptomic specialization across human cortex captured by structural neuroimaging topography. Nature neuroscience 21 (9), 1251.

Collingridge, G.L., Isaac, J.T., Wang, Y.T., 2004. Receptor trafficking and synaptic plasticity. Nature reviews neuroscience 5 (12), 952.

Cools, R., 2019. Chemistry of the adaptive mind: lessons from dopamine. Neuron 104 (1), 113–131.

Das, S., Sasaki, Y.F., Rothe, T., Premkumar, L.S., Takasu, M., Crandall, J.E., Cheung, W., 1998. Increased NMDA current and spine density in mice lacking the NMDA receptor subunit NR3A. Nature 393 (6683), 377.

Economo, M.N., Viswanathan, S., Tasic, B., Bas, E., Winnubst, J., Menon, V., Yao, Z., 2018. Distinct descending motor cortex pathways and their roles in movement. Nature 563 (7729), 79.

Farrant, M., Nusser, Z., 2005. Variations on an inhibitory theme: phasic and tonic activation of GABA A receptors. Nature Reviews Neuroscience 6 (3), 215.

Fritschy, J., Paysan, J., Enna, A., Mohler, H., 1994. Switch in the expression of rat GABAA-receptor subtypes during postnatal development: an immunohistochemical study. Journal of Neuroscience 14 (9), 5302–5324.

Gambrill, A.C., Barria, A., 2011. NMDA receptor subunit composition controls synaptogenesis and synapse stabilization. Proceedings of the National Academy of Sciences 108 (14), 5855–5860.

Geyer, S., Ledberg, A., Schleicher, A., Kinomura, S., Schormann, T., Bürgel, U., Roland, P.E., 1996. Two different areas within the primary motor cortex of man. Nature 382 (6594), 805–807.

Geyer, S., Schleicher, A., Zilles, K., 1999. Areas 3a, 3b, and 1 of human primary somatosensory cortex: 1. Microstructural organization and interindividual variability. Neuroimage 10 (1), 63–83.

Gomez, J., Zhen, Z., Weiner, K.S., 2019. Human visual cortex is organized along two genetically opposed hierarchical gradients with unique developmental and evolutionary origins. PLoS biology 17 (7), e3000362.

Goulas, A., Changeux, J.-P., Wagstyl, K., Amunts, K., Palomero-Gallagher, N., Hilgetag, C.C., 2021. The natural axis of transmitter receptor distribution in the human cerebral cortex. Proceedings of the National Academy of Sciences 118 (3).

Goulas, A., Zilles, K., Hilgetag, C.C., 2018. Cortical gradients and laminar projections in mammals. Trends in Neurosciences 41 (11), 775–788.

Grefkes, C., Geyer, S., Schormann, T., Roland, P., Zilles, K., 2001. Human somatosensory area 2: observer-independent cytoarchitectonic mapping, interindividual variability, and population map. Neuroimage 14 (3), 617–631.

Groc, L., Heine, M., Cousins, S.L., Stephenson, F.A., Lounis, B., Cognet, L., Choquet, D., 2006. NMDA receptor surface mobility depends on NR2A-2B subunits. Proceedings of the National Academy of Sciences 103 (49), 18769–18774.

Hansen, J.Y., Markello, R.D., Tuominen, L., Nørgaard, M., Kuzmin, E., Palomero-Gallagher, N., Misic, B., 2021. Correspondence between gene expression and neurotransmitter receptor and transporter density in the human brain. bioRxiv 2021, 2011. doi:10.1101/2021.11.30.469876, 2030.469876.

Hansen, K.B., Yi, F., Perszyk, R.E., Furukawa, H., Wollmuth, L.P., Gibb, A.J., Traynelis, S.F., 2018. Structure, function, and allosteric modulation of NMDA receptors. The Journal of general physiology 150 (8), 1081–1105.

Hashimoto, T., Arion, D., Unger, T., Maldonado-Aviles, J., Morris, H., Volk, D., Lewis, D., 2008. Alterations in GABA-related transcriptome in the dorsolateral prefrontal cortex of subjects with schizophrenia. Molecular psychiatry 13 (2), 147.

Hawrylycz, M., Miller, J.A., Menon, V., Feng, D., Dolbeare, T., Guillozet-Bongaarts, A.L., Bernard, A., 2015. Canonical genetic signatures of the adult human brain. Nature neuroscience 18 (12), 1832.

Hawrylycz, M.J., Lein, E.S., Guillozet-Bongaarts, A.L., Shen, E.H., Ng, L., Miller, J.A., Jones, A.R., 2012. An anatomically comprehensive atlas of the adult human brain transcriptome. Nature 489, 391. doi:10.1038/nature11405.

Henson, M.A., Roberts, A.C., Salimi, K., Vadlamudi, S., Hamer, R.M., Gilmore, J.H., Philpot, B.D., 2008. Developmental regulation of the NMDA receptor subunits, NR3A and NR1, in human prefrontal cortex. Cerebral Cortex 18 (11), 2560–2573.

Hines, R.M., Davies, P.A., Moss, S.J., Maguire, J., 2012. Functional regulation of GABAA receptors in nervous system pathologies. Current opinion in neurobiology 22 (3), 552–558.

Hörtnagl, H., Tasan, R., Wieselthaler, A., Kirchmair, E., Sieghart, W., Sperk, G., 2013. Patterns of mRNA and protein expression for 12 GABAA receptor subunits in the mouse brain. Neuroscience 236, 345–372.

Kaas, J.H., Hackett, T.A., 2000. Subdivisions of auditory cortex and processing streams in primates. Proceedings of the National Academy of Sciences 97 (22), 11793–11799.

Kujovic, M., Zilles, K., Malikovic, A., Schleicher, A., Mohlberg, H., Rottschy, C., Amunts, K., 2013. Cytoarchitectonic mapping of the human dorsal extrastriate cortex. Brain Structure and Function 218 (1), 157–172.

Lau, C.G., Zukin, R.S., 2007. NMDA receptor trafficking in synaptic plasticity and neuropsychiatric disorders. Nature Reviews Neuroscience 8 (6), 413.

Limon, A., Reyes-Ruiz, J.M., Miledi, R., 2012. Loss of functional GABAA receptors in the Alzheimer diseased brain. Proceedings of the National Academy of Sciences 109 (25), 10071–10076.

Luo, Y., Kusay, A.S., Jiang, T., Chebib, M., Balle, T., 2021. Delta-containing GABA(A) receptors in pain management: Promising targets for novel analgesics. Neuropharmacology 195, 108675. doi:10.1016/j.neuropharm.2021.108675.

Mahfooz, K., Marco, S., Martínez-Turrillas, R., Raja, M.K., Pérez-Otaño, I., Wesseling, J.F., 2016. GluN3A promotes NMDA spiking by enhancing synaptic transmission in Huntington's disease models. Neurobiology of disease 93, 47–56.

Meunier, C.N., Chameau, P., Fossier, P.M., 2017. Modulation of Synaptic Plasticity in the Cortex Needs to Understand All the Players. Frontiers in Synaptic Neuroscience 9, 2. doi:10.3389/fnsyn.2017.00002.

Morosan, P., Rademacher, J., Schleicher, A., Amunts, K., Schormann, T., Zilles, K., 2001. Human primary auditory cortex: Cytoarchitectonic subdivisions and mapping into a spatial reference system. Neuroimage 13 (4), 684–701. doi:10.1006/nimg.2000.0715.

Morosan, P., Schleicher, A., Amunts, K., Zilles, K., 2005. Multimodal architectonic mapping of human superior temporal gyrus. Anat Embryol (Berl) 210 (5-6), 401–406. doi:10.1007/s00429-005-0029-1.

Negi, S.K., Guda, C., 2017. Global gene expression profiling of healthy human brain and its application in studying neurological disorders. Scientific reports 7 (1), 1–12.

Nørgaard, M., Beliveau, V., Ganz, M., Svarer, C., Pinborg, L.H., Keller, S.H., Knudsen, G.M., 2021. A high-resolution in vivo atlas of the human brain's benzodiazepine binding site of GABA(A) receptors. Neuroimage 232, 117878. doi:10.1016/j.neuroimage.2021.117878.

Palomero-Gallagher, N., Zilles, K., 2017. Cortical layers: Cyto-, myelo-, receptor-and synaptic architecture in human cortical areas. Neuroimage.

Palomero-Gallagher, N., Zilles, K., 2018. Cyto-and receptor architectonic mapping of the human brain. In: Handbook of clinical neurology, 150. Elsevier, pp. 355–387.

Palomero-Gallagher, N., Schleicher, A., Bidmon, H.J., Pannek, H.W., Hans, V., Gorji, A., Zilles, K., 2012. Multireceptor analysis in human neocortex reveals complex alterations of receptor ligand binding in focal epilepsies. Epilepsia 53 (11), 1987–1997.

Perez-Otano, I., Larsen, R.S., Wesseling, J.F., 2016. Emerging roles of GluN3-containing NMDA receptors in the CNS. Nat Rev Neurosci 17 (10), 623–635. doi:10.1038/nrn.2016.92.

Pirker, S., Schwarzer, C., Wieselthaler, A., Sieghart, W., Sperk, G., 2000. GABAA receptors: immunocytochemical distribution of 13 subunits in the adult rat brain. Neuroscience 101 (4), 815–850.

Roberts, A.C., Díez-García, J., Rodriguiz, R.M., López, I.P., Luján, R., Martínez-Turrillas, R., Jarrett, T.M., 2009. Downregulation of NR3A-containing NMDARs is required for synapse maturation and memory consolidation. Neuron 63 (3), 342–356.

Rottschy, C., Eickhoff, S.B., Schleicher, A., Mohlberg, H., Kujovic, M., Zilles, K., Amunts, K., 2007. Ventral visual cortex in humans: cytoarchitectonic mapping of two extrastriate areas. Human brain mapping 28 (10), 1045–1059.

Schleicher, A., Amunts, K., Geyer, S., Morosan, P., Zilles, K., 1999. Observer-independent method for microstructural parcellation of cerebral cortex: a quantitative approach to cytoarchitectonics. Neuroimage 9 (1), 165–177.

Sequeira, A., Shen, K., Gottlieb, A., Limon, A., 2019. Human brain transcriptome analysis finds region-and subject-specific expression signatures of GABAAR subunits. Communications biology 2 (1), 1–14.

Sieghart, W., Sperk, G., 2002. Subunit composition, distribution and function of GABA-A receptor subtypes. Current Topics in Medical Chemistry 2 (8), 795–816.

Tasic, B., Yao, Z., Graybuck, L.T., Smith, K.A., Nguyen, T.N., Bertagnolli, D., Viswanathan, S., 2018. Shared and distinct transcriptomic cell types across neocortical areas. Nature 563 (7729), 72.

Van Essen, D.C., Anderson, C.H., Felleman, D.J., 1992. Information processing in the primate visual system: an integrated systems perspective. Science 255 (5043), 419–423.

Wang, X.-J., 2020. Macroscopic gradients of synaptic excitation and inhibition in the neocortex. Nature Reviews Neuroscience 21 (3), 169–178.

Wisden, W., Laurie, D.J., Monyer, H., Seeburg, P.H., 1992. The distribution of 13 GABAA receptor subunit mRNAs in the rat brain. I. Telencephalon, diencephalon, mesencephalon. Journal of Neuroscience 12 (3), 1040–1062.

Zachlod, D., Rüttgers, B., Bludau, S., Mohlberg, H., Langner, R., Zilles, K., Amunts, K., 2020. Four new cytoarchitectonic areas surrounding the primary and early auditory cortex in human brains. Cortex 128, 1–21.

Zeisel, A., Muñoz-Manchado, A.B., Codeluppi, S., Lönnerberg, P., La Manno, G., Juréus, A., Betsholtz, C., 2015. Cell types in the mouse cortex and hippocampus revealed by single-cell RNA-seq. Science 347 (6226), 1138–1142.

Zilles, K., Amunts, K., 2009. Receptor mapping: architecture of the human cerebral cortex. Current opinion in neurology 22 (4), 331–339.

Zilles, K., Amunts, K., 2012. Segregation and wiring in the brain. Science 335 (6076), 1582–1584.

Zilles, K., Palomero-Gallagher, N., Kaas, J.H., 2017. Comparative Analysis of Receptor Types That Identify Primary Cortical Sensory Areas. In: Evolution of Nervous Systems (Second Edition). Academic Press, Oxford, pp. 225–245.

Zilles, K., Palomero-Gallagher, N., 2017. Multiple transmitter receptors in regions and layers of the human cerebral cortex. Frontiers in Neuroanatomy 11, 78.

Zilles, K., Palomero-Gallagher, N., Grefkes, C., Scheperjans, F., Boy, C., Amunts, K., Schleicher, A., 2002. Architectonics of the human cerebral cortex and transmitter receptor fingerprints: reconciling functional neuroanatomy and neurochemistry. European neuropsychopharmacology 12 (6), 587–599.

Zilles, K., Palomero-Gallagher, N., Schleicher, A., 2004. Transmitter receptors and functional anatomy of the cerebral cortex. Journal of anatomy 205 (6), 417–432.

Zilles, K., Schleicher, A., Palomero-Gallagher, N., Amunts, K., 2002. Quantitative analysis of cyto-and receptor architecture of the human brain. In: Brain mapping: the methods. Elsevier, pp. 573–602.